

## The protective role of peroxisome proliferator-activated receptor gamma in lipotoxic podocytes

Almudena G. Carrasco<sup>a</sup>, Adriana Izquierdo-Lahuerta<sup>a,\*</sup>, Ángela M. Valverde<sup>b,c,d</sup>, Lan Ni<sup>e</sup>, Elena Flores-Salguero<sup>a</sup>, Richard J. Coward<sup>e</sup>, Gema Medina-Gómez<sup>a,d,\*\*</sup>

<sup>a</sup> Universidad Rey Juan Carlos, Dpto. de Ciencias Básicas de la Salud, Avda. de Atenas s/n. 28922, Alcorcón, Madrid, Spain

<sup>b</sup> Institute of Biomedical Research "Alberto Sols" (CSIC-UAM), 28029 Madrid, Spain

<sup>c</sup> Centro de Investigación Biomédica en Red de Diabetes y Enfermedades Metabólicas Asociadas (CIBER-dem), ISCIII, 28029 Madrid, Spain

<sup>d</sup> MEMORISM Research Unit of University Rey Juan Carlos-Institute of Biomedical Research "Alberto Sols" (CSIC), Madrid, Spain

<sup>e</sup> Bristol Renal, Translational Health Sciences, University of Bristol, Bristol, UK

### ARTICLE INFO

#### Keywords:

PPARgamma

RXR

Lipid droplets

TZD

Bexarotene

Podocyte

### ABSTRACT

Podocytes are specialized epithelial cells that maintain the glomerular filtration barrier. These cells are susceptible to lipotoxicity in the obese state and irreversibly lost during kidney disease leading to proteinuria and renal injury. PPAR $\gamma$  is a nuclear receptor whose activation can be renoprotective. This study examined the role of PPAR $\gamma$  in the lipotoxic podocyte using a PPAR $\gamma$  knockout (PPAR $\gamma$ KO) cell line and since the activation of PPAR $\gamma$  by Thiazolidinediones (TZD) is limited by their side effects, it explored other alternative therapies to prevent podocyte lipotoxic damage.

Wild-type and PPAR $\gamma$ KO podocytes were exposed to the fatty acid palmitic acid (PA) and treated with the TZD (Pioglitazone) and/or the Retinoid X receptor (RXR) agonist Bexarotene (BX).

It revealed that podocyte PPAR $\gamma$  is essential for podocyte function. PPAR $\gamma$  deletion reduced key podocyte proteins including podocin and nephrin while increasing basal levels of oxidative and ER stress causing apoptosis and cell death. A combination therapy of low-dose TZD and BX activated both the PPAR $\gamma$  and RXR receptors reducing PA-induced podocyte damage. This study confirms the crucial role of PPAR $\gamma$  in podocyte biology and that their activation in combination therapy of TZD and BX may be beneficial in the treatment of obesity-related kidney disease.

### 1. Introduction

Peroxisome proliferator-activated receptors (PPARs) are ligand activated nuclear hormone receptors that control and modulate multiple cellular functions by activation or repression of target genes. PPARs are class 2 nuclear receptors that anchor to retinoid X receptors (RXRs) forming permissive heterodimers, which bind to the PPAR response element (PPRE) in the promoter region of target genes, to control their expression [1]. Among the three isoforms of PPAR (PPAR $\alpha$ , PPAR $\beta/\delta$

and PPAR $\gamma$ ), PPAR $\gamma$  is a master regulator of adipogenesis and fat storage in adipose tissue through transcriptional regulation of various genes. In addition, PPAR $\gamma$  modulates a broad range of pathophysiological processes, including insulin sensitization, cellular differentiation, and cancer mitosis [1,2]. In humans, the PPAR $\gamma$  gene is located on chromosome 3, and 4 splice variants are generated by alternative splicing and differential promoter usage [3,4]. However, only two protein isoforms ( $\gamma$ 1 and  $\gamma$ 2) are encoded. PPAR $\gamma$ 1 is widely expressed in tissues, including white and brown adipose tissue, skeletal muscle, liver, pancreatic cells,

**Abbreviations:** ABCA1, ATP Binding Cassette Subfamily A Member 1; AKT, protein kinase B; BX, Bexarotene; COX-2, Cyclooxygenase 2; CPT1, carnitine palmitoyltransferase 1; FAS, Fatty acid synthase; GLUT-4, glucose transporter-4; I, Insulin; PGC1, peroxisome proliferator-activated receptor gamma coactivator 1; SREBP1, sterol regulatory element-binding protein 1; FXR, Farnesoid X receptor; LXR, liver X receptor; RAR, retinoic acid receptor; RXR, Retinoid X Receptor; PA, Palmitic acid; PLIN2, Perilipin 2; PPAR, peroxisome proliferator-activated receptor; RBP, retinol binding protein; TGF $\beta$ 1, Transforming Growth factor  $\beta$ 1; TZD, Thiazolidinedione; VDR, Vitamin D receptor; Vh, Vehicle.

\* Corresponding author.

\*\* Correspondence to: G. Medina-Gómez, MEMORISM Research Unit of University Rey Juan Carlos-Institute of Biomedical Research "Alberto Sols" (CSIC), Madrid, Spain.

E-mail addresses: [adriana.izquierdo@urjc.es](mailto:adriana.izquierdo@urjc.es) (A. Izquierdo-Lahuerta), [gema.medina@urjc.es](mailto:gema.medina@urjc.es) (G. Medina-Gómez).

<https://doi.org/10.1016/j.bbalip.2023.159329>

Received 26 December 2022; Received in revised form 16 March 2023; Accepted 20 April 2023

Available online 6 May 2023

1388-1981/© 2023 The Authors. Published by Elsevier B.V. This is an open access article under the CC BY license (<http://creativecommons.org/licenses/by/4.0/>).

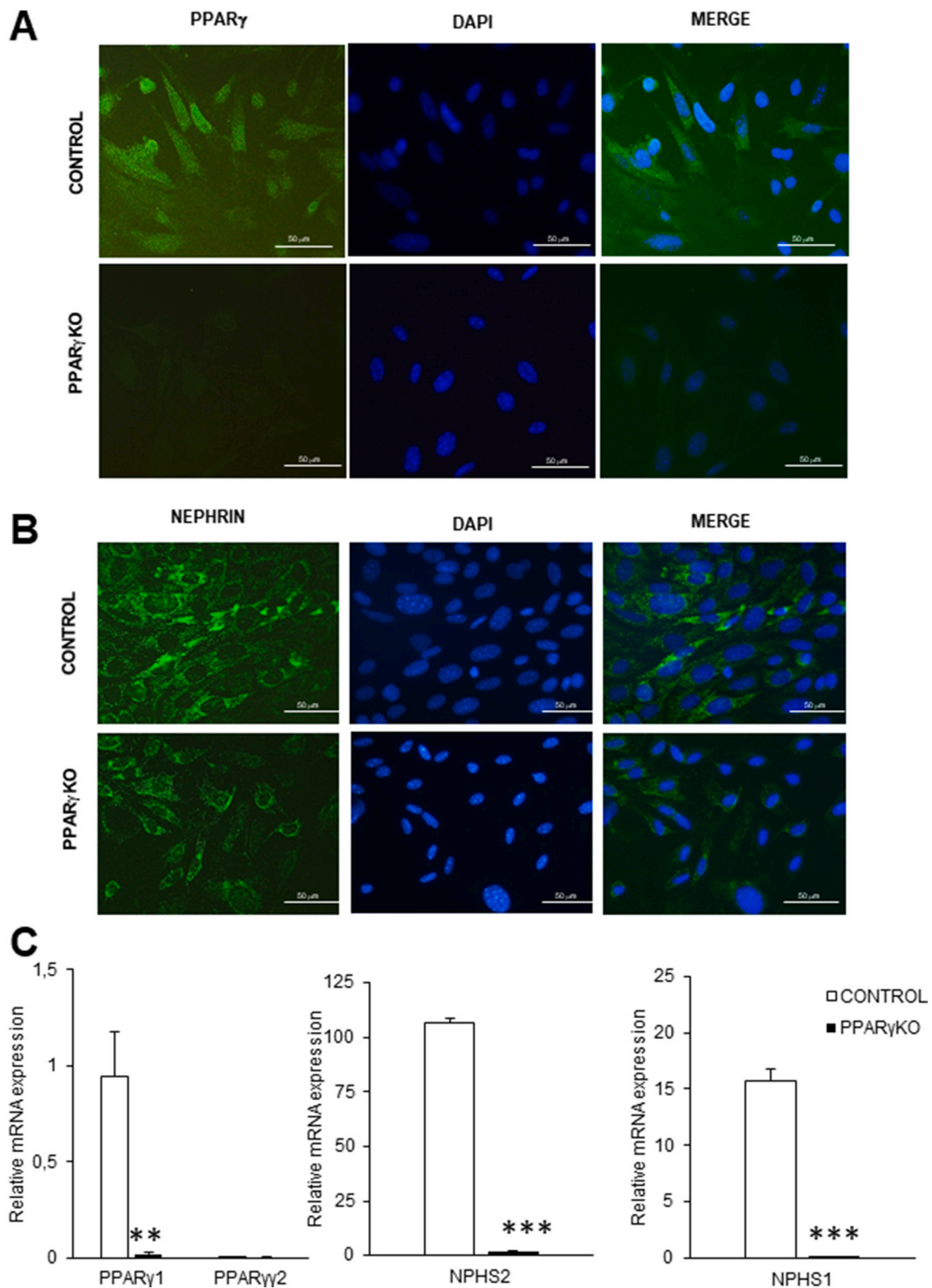


**Fig. 1.** PPAR $\gamma$  is essential for the proper functioning of the podocyte. Representative micrographs of the immunofluorescence for (A) PPAR $\gamma$  and (B) Nephrin in control and PPAR $\gamma$ KO podocytes, Magnification 400 $\times$ . (C) Relative mRNA expression of PPAR $\gamma$ 1 and 2, Podocin (NPHS2) and Nephrin (NPHS1) in control and PPAR $\gamma$ KO podocytes. Data are shown as mean  $\pm$  SEM ( $n = 3$ ). \*\* $p < 0.005$  versus Control podocytes; \*\*\* $p < 0.001$  versus Control podocytes.

macrophages, colon, bone, placenta and kidney [4]. By contrast, PPAR $\gamma$ 2 expression is restricted. It is found in white and brown adipose tissue under physiological conditions, although it can be induced in other tissues in response to overnutrition or genetic obesity.

Recently, it has been shown that PPAR $\gamma$  is crucial in renal metabolism (glucose, lipid and mineral metabolism) [4]. Our group has previously studied the POKO mouse model of the metabolic syndrome generated by ablation of the PPAR $\gamma$ 2 isoform in a leptin-deficient obese

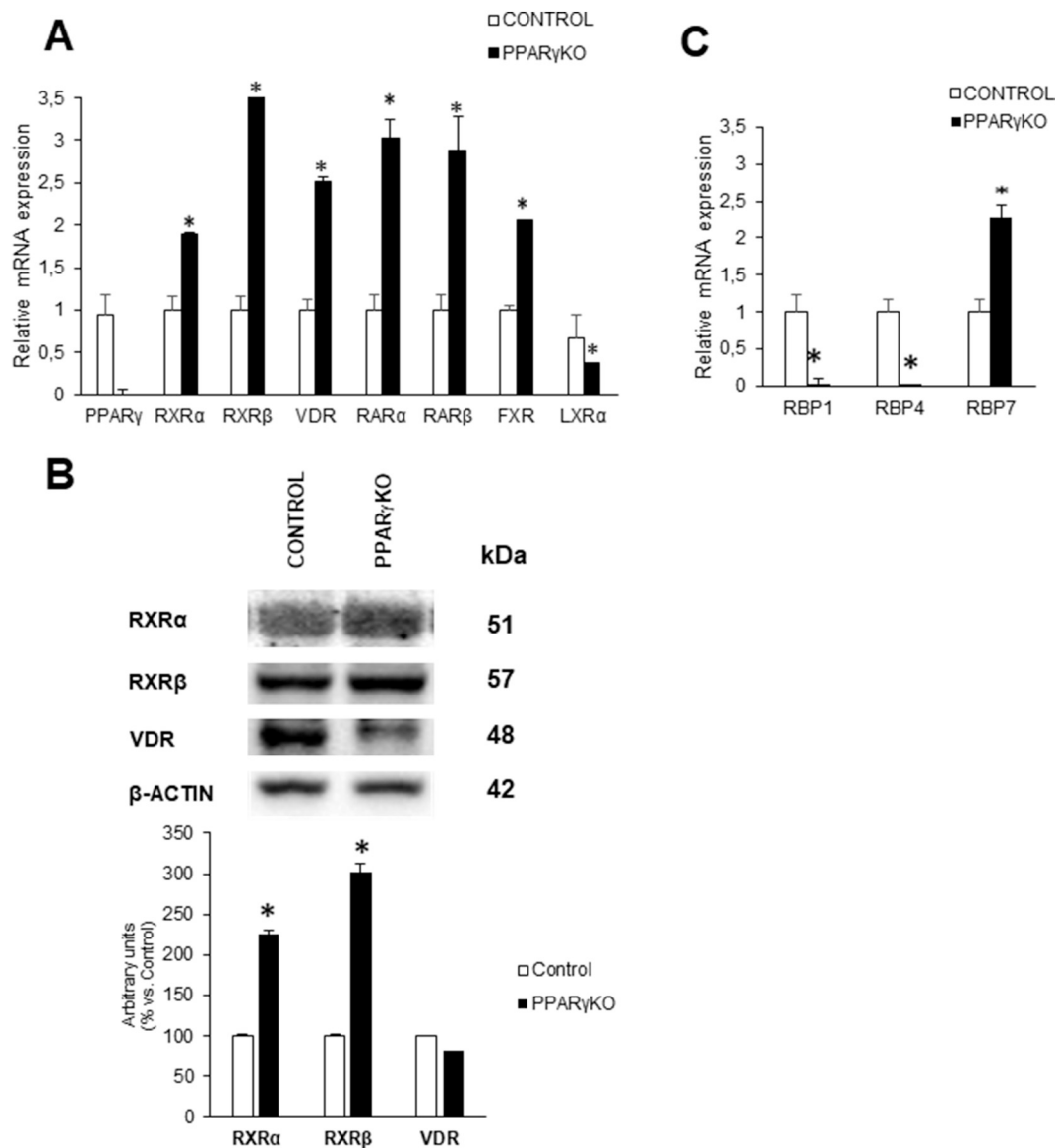


**Fig. 2.** Relative mRNA expression (A) and protein expression (B) of Nuclear Receptor genes and Retinol Binding Proteins (C) in Control and PPAR $\gamma$ KO podocytes. FXR, Farnesoid X receptor; LXR, liver X receptor; PPAR, peroxisome proliferator-activated receptor; PGC1, peroxisome proliferator-activated receptor gamma coactivator 1. RAR, retinoic acid receptor; RBP1, retinol binding protein 1; RBP4, retinol binding protein 1; RBP7: retinol binding protein 7; RXR, Retinoid X Receptor. Data are shown as mean  $\pm$  SEM ( $n = 3$ ). \* $p < 0.05$  versus Control podocytes.

(*ob/ob*) background. This model exhibits accelerated renal damage due to glucolipotoxic effects associated with the metabolic syndrome and insulin resistance [5]. Several renal cell types have endogenous PPAR $\gamma$  expression, including mesangial, renal microvascular endothelial cells and podocytes [4]. Podocytes are key cells in maintaining the integrity of the glomerular filtration barrier. They are insulin sensitive cells (Welsh Cell metabolism reference) and affected by lipotoxic processes [6]. Previous work by our group showed palmitic acid (PA) induces podocyte damage characterized by insulin resistance, inflammation, oxidative and endoplasmic reticulum (ER) stress [7]. Furthermore, it has been shown that the podocyte-specific PPAR $\gamma$ -deficient mice challenged with nephrotoxin develop glomerulonephritis with crescent formation, which is not alleviated by the administration of thiazolidinedione (TZD), an agonist of PPAR $\gamma$  [8].

TZD are used as antidiabetic drugs, and they have renoprotective effects [9]. TZDs administration has been shown to reduce proteinuria in acute nephrotic syndrome through the regulation of  $\alpha$ -actinin-4 and nephrin in a PPAR $\gamma$ -dependent manner [9]. Pioglitazone belongs to the

thiazolidinedione class and has been used for the treatment of type 2 diabetes mellitus (T2DM) to improve glycemic levels. Pioglitazone has been shown to alleviate the renal damage by reducing renal fibrosis, oxidative stress and inflammation in obese rats [10]. Importantly, this effect is independent of improvement in glycemic control or body weight of the animals. When tested in vitro in a podocyte cell line, pioglitazone restored the apoptosis and necrosis damage caused by the administration of puromycin aminonucleoside (PAN) [11]. It also restored the expression of differentiation markers of podocytes in conditionally immortalized cell lines and isolated glomeruli [11,12]. Pioglitazone has also been shown to increase mitochondrial numbers and function in nutrient deprived immortalized human podocytes [13]. Among other nuclear receptors ligands, agonists of retinoic acid or the retinoid receptors (RXR) have also been shown to have renoprotective effects as well as promote normal renal development through the action of vitamin A [14].

Unfortunately, PPAR $\gamma$  agonists have significant side effects, especially when administered at high doses [15]. Therefore, combination of

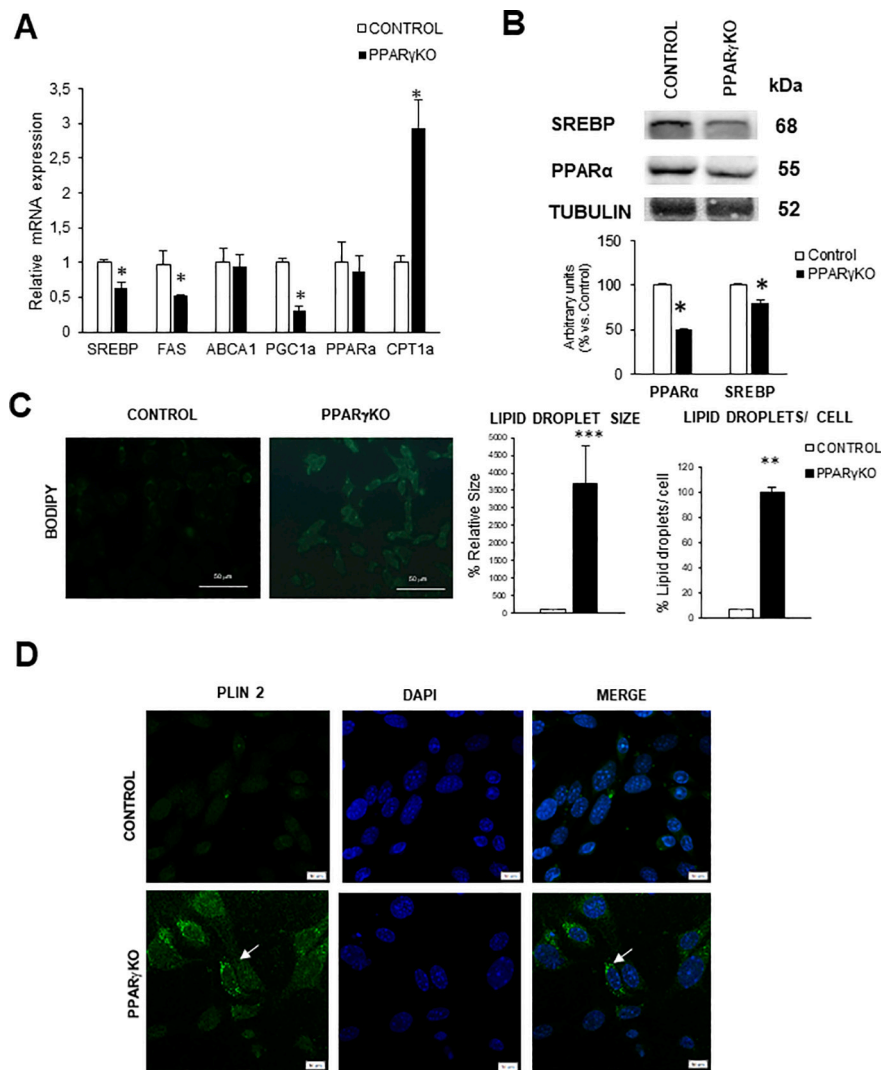


**Fig. 3.** Lipidic metabolism is dysregulated in PPAR $\gamma$ KO podocytes. Relative mRNA expression (A) and protein expression (B) of lipid metabolism genes: ABCA1, ATP Binding Cassette Subfamily A Member 1; CPT1, carnitine palmitoyltransferase 1; FAS, Fatty acid synthase; PPAR, peroxisome proliferator-activated receptor; SREBP1, sterol regulatory element-binding protein 1. Data are shown as mean  $\pm$  SEM (n = 3). \**p* < 0.05 versus Control podocytes. C: Representative BODYPI staining in podocytes and colour quantification after dye elution, (n = 3 experiments); original magnification: 400 $\times$ . D: Representative photographs of immunohistochemistry of Perilipin 2 (n = 3 experiments); White arrows show perilipin 2 in lipid droplets inside podocytes. Original magnification: 400 $\times$ .

these agonists with other molecules has been explored [16–18]. Finally, pioglitazone has been also combined with the RXR agonist bexarotene in the treatment of lung cancer, exhibiting synergistic effects [19,20] supporting its combined use in this work.

In this study, we used an *in vitro* approach to understand the role of PPAR $\gamma$  in the lipotoxic podocyte. Furthermore, we explored the benefit of combining PPAR $\gamma$  and RXR ligands in this renal cell type.

## 2. Materials and methods

### 2.1. Cell lines, culture and treatments

To generate a conditionally immortalized mouse PPAR $\gamma$  floxed podocyte cell line, we obtained the kidneys from PPAR $\gamma$  floxed mice [21] kindly provided by Frank J. Gonzalez (Laboratory of Metabolism, National Cancer Institute, National Institutes of Health, Bethesda, MD, USA). From these kidneys, a conditionally immortalized PPAR $\gamma$  floxed podocyte line was engineered as done previously [22,23]. The cell line was maintained in RPMI 1640 Sigma-Aldrich (St. Louis, MO, USA) supplemented with 10 % FBS and penicillin (100 U/mL)/streptomycin (100  $\mu$ g/mL). The PPAR $\gamma$  floxed podocyte line proliferates at 33  $^{\circ}$ C and becomes quiescent and differentiates when thermo-shifted to 37  $^{\circ}$ C. Differentiation requires 10–14 days.

To achieve PPAR $\gamma$  deletion,  $3 \times 10^4$  podocytes PPAR $\gamma$  floxed were seeded on 6-well plate, 12h after plating cells were infected with 200

MOI of Cre recombinase adenovirus vector (Vector Biolabs) in 200  $\mu$ l RPMI with 10 % FBS, 1 h after addition of viral particles the media was supplemented with 400  $\mu$ l medium and 10 % FBS. After 24 h, the medium was changed, and cells were allowed to grow for 72 h. Subsequently, Real time PCR and immunofluorescence was used to select the clone with the lowest expression of PPAR $\gamma$  1 and 2, and it was subcloned to obtain PPAR $\gamma$ KO podocytes (Fig. 1A).

All experiments were performed after 12 h of serum starvation. Passage numbers 6 to 12 were used for all experiments and were performed at least 3 times.

Palmitate (PA) treatment was performed as described previously [7]. Briefly, 20 % fatty acid-free BSA solution was heated to 37  $^{\circ}$ C before the addition of a 100 mM PA stock solution dissolved in ethanol. The solution was heated to 37  $^{\circ}$ C until clear and diluted with RPMI 1640 to give a final concentration of 5 % BSA, 1 % ethanol and 500  $\mu$ M PA. The solution was filter sterilized (0.2  $\mu$ m pore size) before being added onto the cells. The control for palmitate (vehicle) was RPMI 1640, 5 % fatty acid-free BSA and 1 % ethanol.

Bexarotene from LC Laboratories (Woburn, MA, USA) was added at 1  $\mu$ M to RPMI with PA (500  $\mu$ M) by 24 h. Pioglitazone (Takeda-Lilly, Madrid, Spain) was added at 0.1  $\mu$ M to RPMI with PA (500  $\mu$ M) by 24 h. The combined therapy consisted in Bexarotene 0.5  $\mu$ M and Pioglitazone 0.05  $\mu$ M add to RPMI with PA (500  $\mu$ M) by 24 h.

To perform the insulin stimulation assay, differentiated podocytes were maintained in serum-free medium for 18 h. Then the cells were

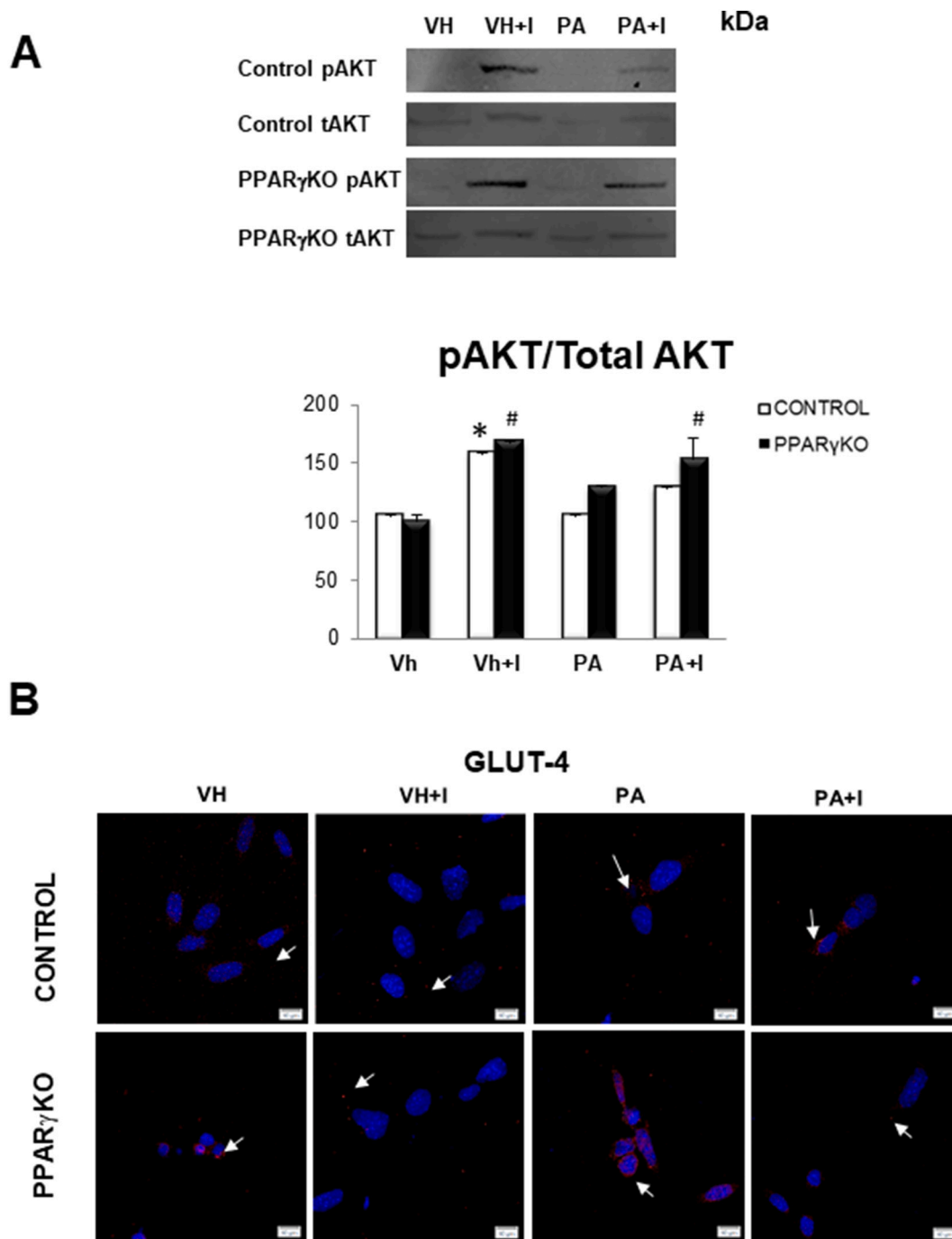


**Fig. 4.** PPAR $\gamma$ KO podocytes do not develop insulin resistance in the presence of palmitic acid. **A:** Representative immunoblot and quantification of pAkt(Ser473) protein extracts of PA-treated podocytes plus 100 nM insulin. Levels were normalized to total protein kinase B (tAkt), i.e., pAkt/tAkt; ( $n = 3$  experiments); \* $p < 0.05$  versus VH of Control podocytes; # $p < 0.05$  versus VH of PPAR $\gamma$ KO podocytes. **B:** Representative photographs of immunohistochemistry of glucose transporter-4 (GLUT 4) ( $n = 3$  experiments); White arrows show GLUT4 in cytoplasm or translocated to membrane by insulin signaling. Original magnification: 400 $\times$ ; VH: Vehicle; I: Insulin; PA: Palmitic acid.

incubated without or with PA (500  $\mu$ M) plus treatment for 24 h. Subsequently, cells were washed, and insulin was added for 5–10 min to a final concentration of 100 nM.

## 2.2. mRNA extraction and quantitative RT-PCR

RNA extraction, quantification and retro-transcription was performed as described [5]. cDNA was also prepared from the conditionally immortalized mouse podocyte cell line, used for in vitro experiments. All quantitative RT-PCR assays were performed in duplicate for each

sample.  $\beta$ -actin, 36b4 and 18s were used as housekeeping genes. To validate housekeeping genes, we used the BestKeeper software tool [24]. All primers are listed in Table S1.

## 2.3. Protein extraction and Western blotting

The cells were washed twice with ice cold PBS and scraped into RIPA buffer plus protein inhibitors. The protein concentration was determined by Bradford method. Proteins were separated on 10 or 12 % SDS-PAGE and transferred to nitrocellulose membranes. Membranes were



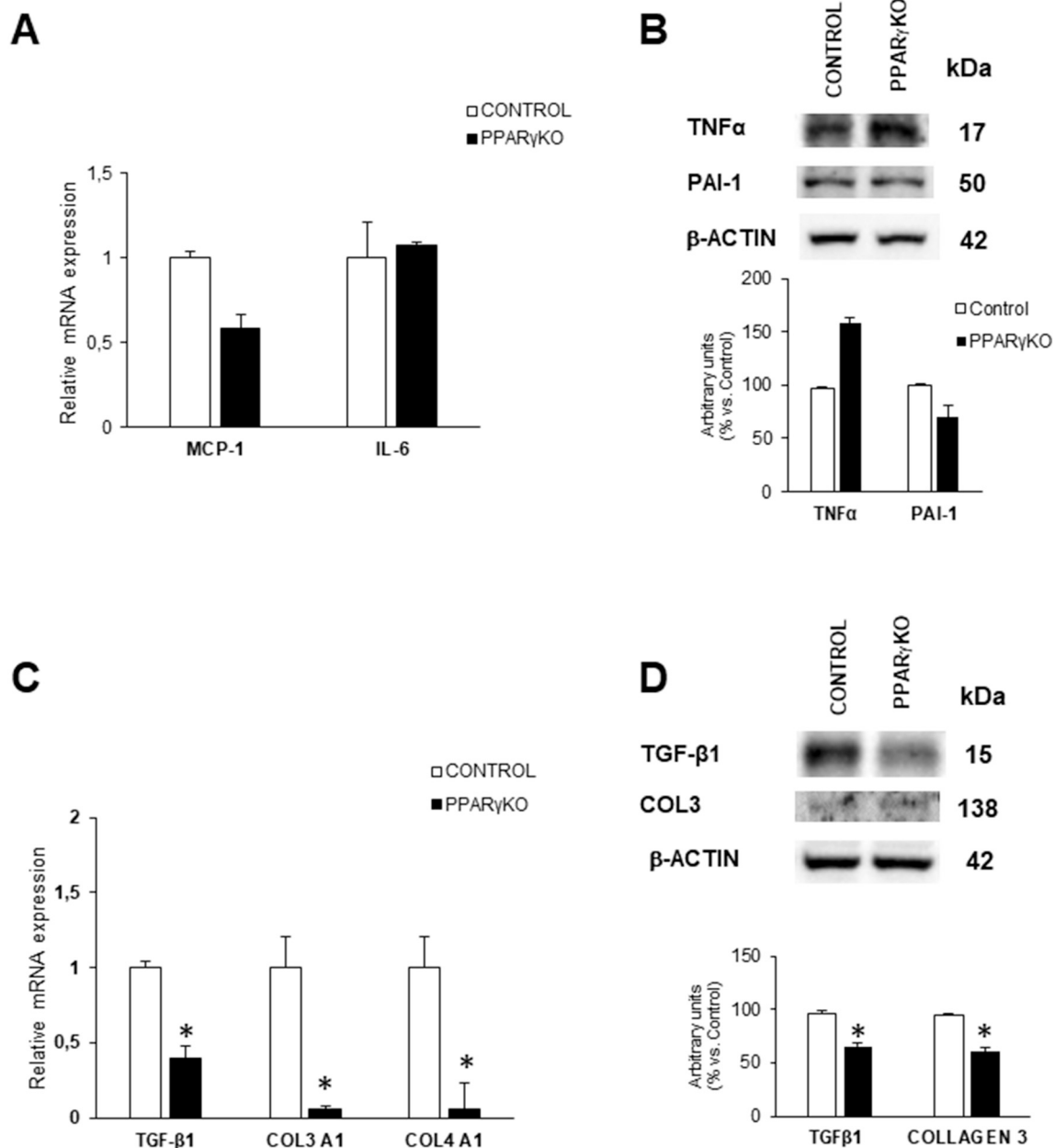


**Fig. 5.** Relative mRNA expression and protein expression related with inflammation (A and B) and Fibrosis (C and D) in Control and PPAR $\gamma$ KO podocytes. A: Relative mRNA expression of genes related with inflammation; B: Protein expression related with inflammation; C: Relative mRNA expression of genes related with fibrosis; D: Protein expression of genes related with fibrosis in Control and PPAR $\gamma$ KO podocytes. COL: Collagen; IL-6: Interleukin 6; MCP-1: Monocyte chemoattractant protein 1; TGF $\beta$ 1: Transforming Growth factor  $\beta$ 1. Data are shown as mean  $\pm$  SEM (n = 3). \*p < 0.05 versus Control podocytes.

blocked and probed with the following antibodies: anti- $\beta$ -actin (Sigma), anti-Bcl-2, anti-PAI-1, anti-SREBP, anti-TNF $\alpha$  and anti-VDR (SantaCruz); anti-collagen 3, anti-RXR $\alpha$ , anti-RXR $\beta$ , anti-podocin and anti-TGF- $\beta$ 1 (Abcam Inc.); anti-PPAR $\alpha$  (ThermoFisher); anti-phospho-AKT (Ser) and anti-total-AKT (Cell Signaling). The protein band density was measured using the ImageJ 1.45 software (National Institutes of Health, Bethesda, MD). The amount of protein under control conditions was assigned a relative value of 100 %.

#### 2.4. Measurement of superoxide production

The effect of PA on superoxide production dihydroethidium (DHE; Sigma, St. Louis, Mo) was performed with a method described by Jiménez-Altayó et al. [25]. Dihydroethidium (DHE) is a fluorescent superoxide-anion probe (Beyotime, China). Following uptake by living

cells, intracellular superoxide anions act on DHE to dehydrogenate it to ethidium that combines with DNA or RNA to generate red fluorescent DHE. DHE fluorescence occurs at excitation wavelength of 488 nm and an emission wavelength of 535 nm. Podocytes were seeded on coverslips in 24-well plates and treated for 24 h with vehicle or PA plus treatment. Then, cells were exposed to 10  $\mu$ M DHE dissolved in RPMI 1640 for 30 min at 37  $^{\circ}$ C. To analyze the changes in fluorescence by PA treatment, we assigned 1 point to vehicle fluorescence emission. Fluorescence was measured using a 40 $\times$  objective of a fluorescence microscope (Axiophot Zeiss). Then, we quantified the red fluorescence of all nuclei found per image (3 coverslips per treatment/3 fields/6 photographs of each) using image software AxioVision Software 4.6, Carl Zeiss. (N = 3 experiments).

We used MitoSOX-based flow cytometry for detection mitochondrial ROS production in podocytes. MitoSOX Red (Invitrogen, Grand Island,

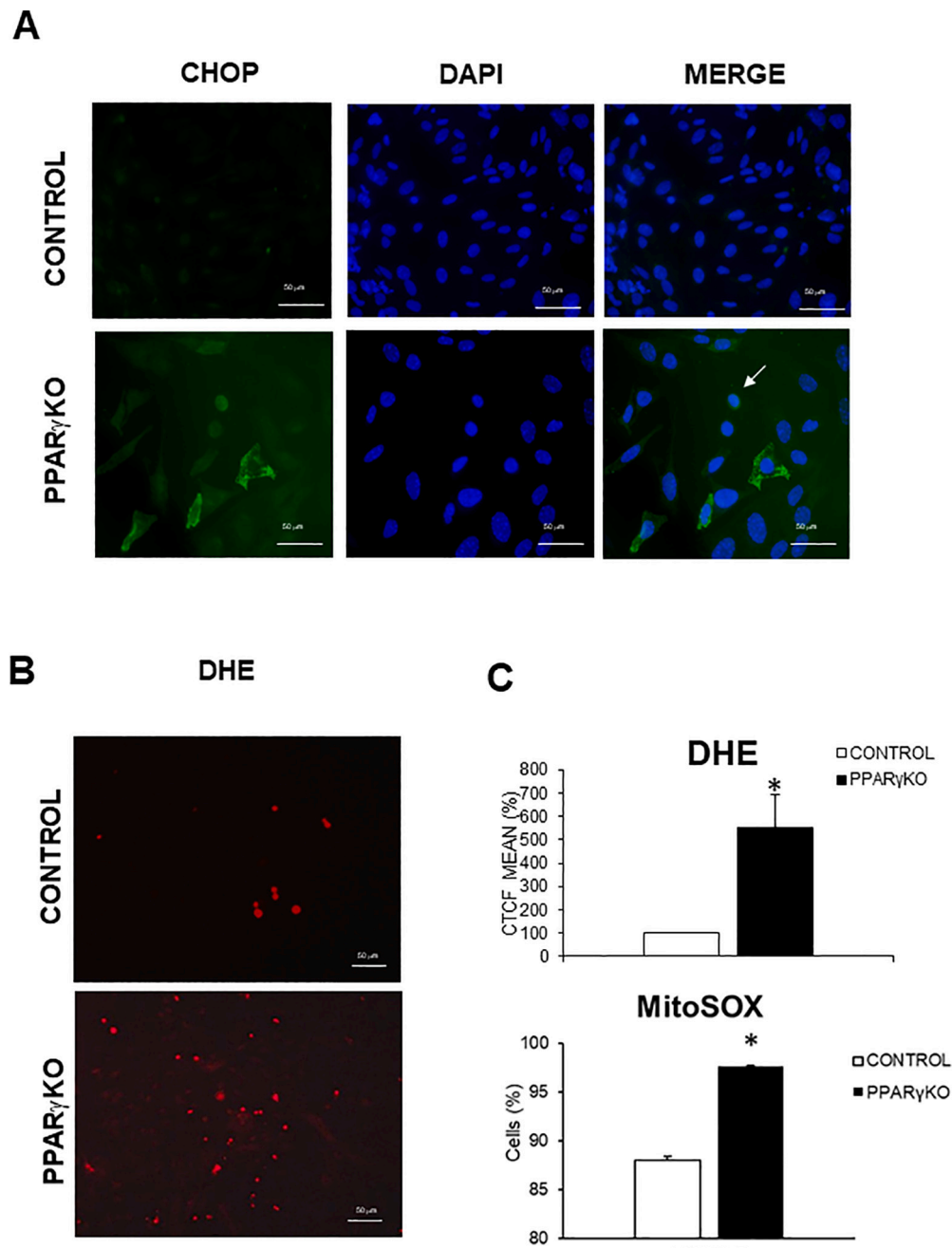


**Fig. 6.** PPAR $\gamma$ KO podocytes presented an increased RE stress and ROS production. A: Representative micrographs of the immunofluorescence for c/EBP homologous protein (CHOP) in Control and PPAR $\gamma$ KO podocytes (white arrows at stained nuclei). Magnification 400 $\times$ . B: Representative photographs of the nuclei of podocytes incubated with Di-hydroethidium (DHE) probe and red fluorescence MitoSOX quantification by flow cytometry ( $n = 3$  experiments); Original magnification: 200 $\times$ .

NY) is a modified DHE analog derived by the addition of a triphenylphosphonium group, which specifically detect mitochondrial superoxide in mitochondria. 50,000 events from each condition ( $N = 3$  experiments) were measured through flow cytometry (Beckman Coulter Cytomics FC500 MPL) and percentage of marked cells analyzed and quantified based on the modification to the protocol proposed by Kauffman et al. [26].

#### 2.5. Measurement of cellular viability and quantification of apoptosis and necrosis

This was determined with propidium iodide (PI) staining and fluorescently labeled annexin V through the FITC Annexin V/Dead Cell Apoptosis Kit (V13242, Invitrogen, USA) by flow cytometry. PI is

impermeant to live cells and apoptotic cells, but stains dead cells with fluorescence, binding tightly to the nucleic acids in the cell. After staining a cell population with FITC annexin V and PI, apoptotic cells show green fluorescence, dead cells show red and green fluorescence and live cells show little or no fluorescence. These populations can easily be distinguished using a flow cytometer with the 488 nm line of an argon-ion laser for excitation. This way, 50,000 events from each condition ( $N = 3$  experiments) were measured through flow cytometry (Beckman Coulter Cytomics FC500 MPL) and percentage of marked cells analyzed and quantified.

#### 2.6. Measurement of lipid accumulation

Measurement of lipid accumulation in podocytes was determined by

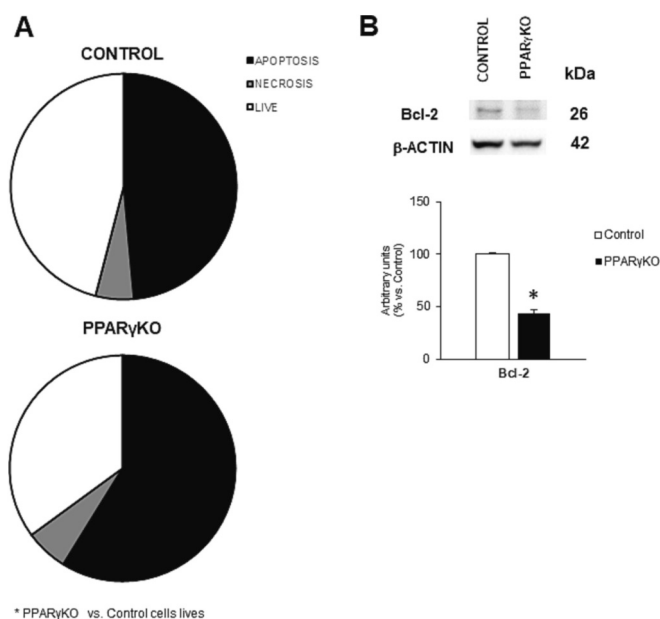


**Fig. 7.** PPAR $\gamma$ KO podocytes presented a decline in cellular viability and an increased death by apoptosis. A: Representation of percentage of cell lives and death by apoptosis or necrosis measured with propidium iodide staining and annexin V by flow cytometry; B: Protein expression of antiapoptotic protein B-cell lymphoma 2 (Bcl-2). \* $p < 0.05$  vs. Control podocytes.

a fluorometric assay using BODIPY<sup>TM</sup> (4,4-difluoro-3a,4-diaza-s-indacene) probe 493/603 (Invitrogen). BODIPY is commonly used to detect intracellular neutral lipids, emitting a maximum fluorescence of 510 nm at 665 nm. Podocytes were seeded on coverslips in 24-well plates and treated for 24 h with vehicle or PA, with or without BX and TZD. Then, cells were exposed to 50 ng/ml BODIPY dissolved in RPMI 1640 for 30 min at 37 °C. Fluorescence was measured using a 40 $\times$  objective of a fluorescence microscope (Axiophot Zeiss). Finally, we quantified the green fluorescence of all cell and lipid droplets found per image (3 coverslips per treatment/3 fields/6 photographs of each) using image software AxioVision Software 4.6, Carl Zeiss. ( $N = 3$  experiments).

## 2.7. Immunofluorescence

Podocytes grown on cover slips were fixed with 4 % paraformaldehyde. After blocking, cells were incubated with anti-Nephrin (Abcam Inc.), anti-Podocin (Abcam Inc.), anti-CHOP, anti-GLUT-4 (Millipore) and anti-Perilipin 2 (Santa Cruz Biotechnology, Inc.). Secondary antibodies were FITC-conjugated. Some samples were incubated without the primary antibodies to serve as negative controls. The nuclei were visualized using DAPI dye. Photographs were captured using an inverted fluorescence microscope (ECLIPSE 90i (Nikon Instruments Europe B.V.) and Confocal microscope (FV 3000 Olympus)). GLUT4 images of podocytes were assessed by two independent blinded observers who scored at least 100 cells per condition for cytoplasmic or peripheral localization.

## 2.8. Statistical analysis

Results are expressed as mean  $\pm$  S.E.M. (standard error of the mean). Statistical differences and interactions were evaluated through a one-way or two-way factorial analysis of variance (ANOVA) using Kruskal-Wallis test. When statistically significant differences resulted at the interaction level, Student's- $t$  or Mann-Whitney tests were carried out to compare the experimental data two by two. Differences were considered statistically significant at  $p < 0.05$ . The program used was GraphPad

InStat (GraphPad Software, Inc.).

## 3. Results

### 3.1. PPAR $\gamma$ is essential for survival and maintaining podocyte homeostasis

#### 3.1.1. PPAR $\gamma$ is essential for the expression of key podocyte proteins and nuclear receptors

Wild-type (WT) podocytes expressed PPAR $\gamma$ 1, while PPAR $\gamma$ 2 expression was practically undetectable (Fig. 1A and C). Deletion of PPAR $\gamma$  in podocytes (PPAR $\gamma$ KO) decreased the expression of key podocyte proteins, essential for the establishment of slit diaphragm and the integrity of the glomerular filtration barrier (GFB) in the kidney, including nephrin (Fig. 1B and C) and podocin (Fig. 1C) compared with WT controls.

As PPAR $\gamma$  is a nuclear receptor that forms heterodimers with RXR, we explored if PPAR $\gamma$  deletion affected the nuclear expression balance in PPAR $\gamma$ KO podocytes. Nuclear receptors that heterodimerize with PPAR $\gamma$ , such as RXR $\alpha$  and RXR $\beta$ , together with those that dimerize with RXR, such as Retinoic Acid receptor  $\alpha$  (RAR $\alpha$ ), RAR $\beta$ , Farnesoid X receptor (FXR) and Vitamin D receptor (VDR) were assessed (Fig. 2A). Most receptors were overexpressed in a constitutive way in PPAR $\gamma$ KO podocytes compared with WT-controls. Liver X receptor  $\alpha$  (LXR $\alpha$ ) was the exception with decreased expression in the PPAR $\gamma$ KO podocytes (Fig. 2A).

The mRNA expression of proteins related to the metabolism of retinoic acid such as the retinol binding proteins (RBP1, RBP4 and RBP7) were also assessed, as they are PPAR $\gamma$  targets [27–29]. RBP1, a cellular protein which stores retinol (vitamin A) and retinal at cellular level, and RBP4, that transports retinol in the blood, were absent in PPAR $\gamma$ KO podocytes compared to the WT-control podocytes, while the RBP7, a cellular protein involved in lipid and whole-body energy metabolism, was increased (Fig. 2A).

#### 3.1.2. PPAR $\gamma$ is crucial for the regulation of lipid homeostasis in the podocyte

Due to PPAR $\gamma$  role in lipid metabolism, we analyzed the expression of multiple genes and proteins involved in lipid synthesis (Fig. 3A and B), including Fatty Acid Synthase (FAS) and Sterol Regulatory Element-binding Protein (SREBP). We also studied lipid oxidation genes, such as Peroxisome Proliferator-Activated Receptor gamma Coactivator 1 (PGC1 $\alpha$ ), PPAR $\alpha$  and Carnitine palmitoyltransferase 1- $\alpha$  (CPT1 $\alpha$ ). ATP Binding Cassette Subfamily A Member 1 (ABCA1) (Fig. 3A and B). Loss of PPAR $\gamma$  significantly decreased levels of genes involved in lipid synthesis (SREBP and FAS). However, changes were not so clear in lipid oxidation, where PGC1 $\alpha$  decreased, CPT1 $\alpha$  increased and PPAR $\alpha$  did not change. No changes were observed in ABCA1 mRNA expression.

We also assessed PPAR $\gamma$ 's role in lipid droplets formation in the podocytes. We analyzed the size and number of lipid droplets by a fluorometric assay using BODIPY in both cell lines. PPAR $\gamma$ KO podocytes had significantly increased numbers of large droplets compared to control podocytes (Fig. 3C). This effect was accompanied by an increase of Perilipin 2 (PLIN2), a protein involved in the formation and stability of the lipid droplets, in PPAR $\gamma$ KO podocytes (Fig. 3D).

#### 3.1.3. Deletion of PPAR $\gamma$ prevents PA-induced insulin resistance through decreased fibrosis

Since PPAR $\gamma$  also regulates the expression of genes involved in glucose metabolism, we assessed if the deletion of PPAR $\gamma$  had any effect on insulin sensitivity. In basal conditions the PPAR $\gamma$ KO podocytes exhibited an increase in PI3K signaling as shown by the ratio of insulin stimulated pAKT/tAKT (Fig. 4A) and increased translocation of the glucose transporter 4 (GLUT 4) from the cytoplasm to the cell membrane (Fig. 4B). Under PA conditions control podocytes had a reduced insulin stimulated pAKT/tAKT levels, together with lack of translocation of



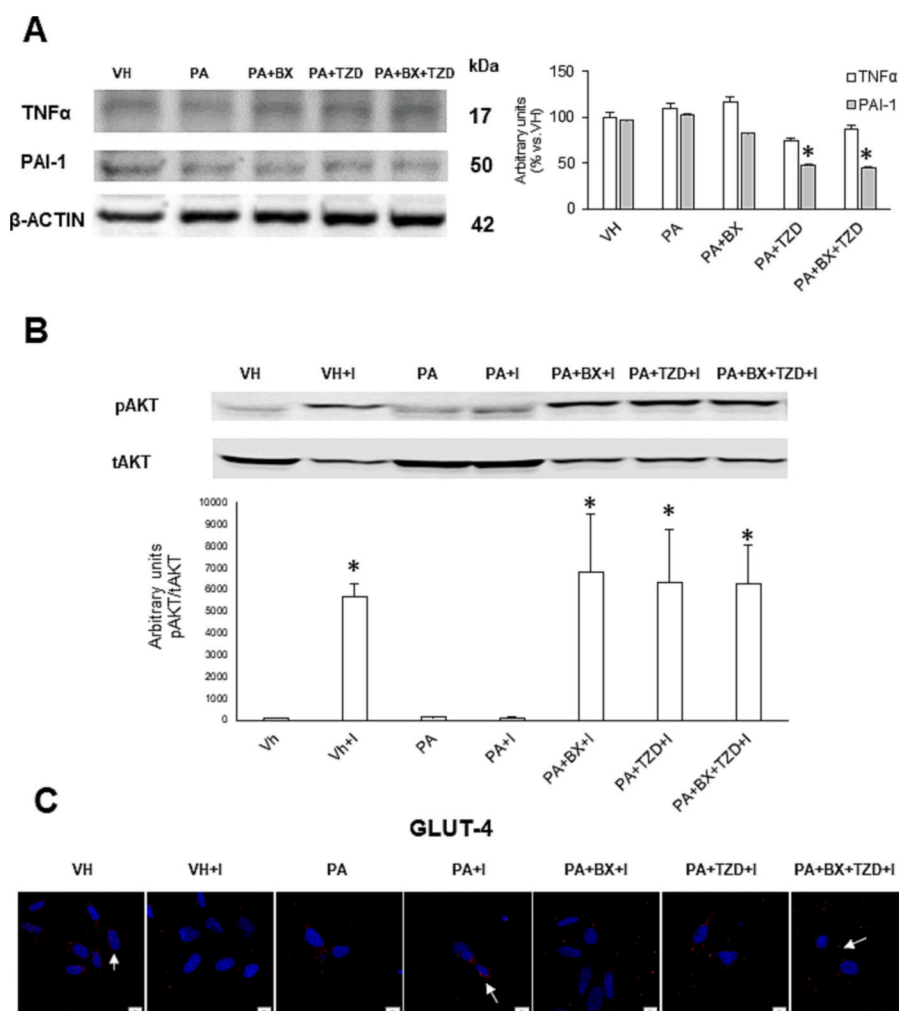


**Fig. 8.** TZD and BX recover the changes in glucose metabolism, insulin resistance and inflammation in podocytes treated with PA. A: Protein expression of inflammatory related genes: TNF $\alpha$  and PAI-1 in podocytes treated 24 h with vehicle, PA, and TZD, BX. B: Representative immunoblot and quantification of pAkt(Ser473) protein extracts of PA-treated podocytes plus 100 nM insulin. Levels were normalized to total protein kinase B (tAkt), i.e., pAkt/tAkt; ( $n = 3$  experiments). C: Representative photographs of immunohistochemistry of glucose transporter-4 (GLUT 4) ( $n = 3$  experiments); White arrows show GLUT4 in cytoplasm or translocated to membrane by insulin signaling. Original magnification: 400 $\times$ ; \* $p < 0.05$  versus VH; BX: Bexarotene; I: Insulin; PA: Palmitic acid; PAI-1: Plasminogen activator inhibitor type 1; TNF $\alpha$ : Tumor necrosis factor alpha; TZD: Thiazolidinedione.

GLUT-4 to the membrane in response to insulin compared to basal conditions. Interestingly, PPAR $\gamma$ KO podocytes exposed to PA had a marked increase in the pAkt/tAkt levels (Fig. 4A) and GLUT4 plasma membrane translocation in response to insulin suggesting increased insulin sensitivity in this situation (Fig. 4B).

Under basal conditions, the mRNA expression of inflammatory markers, Interleukin-6 (IL-6) and Monocyte chemoattractant protein 1 (MCP-1) and protein levels of TNF $\alpha$  and PAI-1 by Western blot, were unchanged in PPAR $\gamma$ KO compared to control podocytes (Fig. 5A and B).

Despite no effect on inflammation, we also wanted to know the effect of PPAR $\gamma$  deletion on fibrosis-related proteins. Transforming Growth factor  $\beta$ 1 (TGF $\beta$ 1) and Collagen 3 had decreased mRNA and protein expression in the PPAR $\gamma$ KO podocytes compared with control podocytes (Fig. 5C and D).

### 3.1.4. Deletion of PPAR $\gamma$ increases ROS production, ER stress and apoptosis in podocytes

At baseline, PPAR $\gamma$ KO podocytes showed increased translocation of CHOP (CCAAT/enhancer-binding protein homologous protein), a marker of ER stress, to the nucleus compared to control podocytes (Fig. 6A). This increase was accompanied by a significant increase in ROS production, measured by Di-hydroethidium (DHE) and MitoSOX probe in the PPAR $\gamma$ KO podocytes under basal conditions (Fig. 6B). We also observed a significant increase in cell death due to increased apoptosis, but not necrosis (Fig. 7).

### 3.2. The use of a combination therapy promotes a reduction of PA induced damage in podocytes

We treated PPAR $\gamma$ KO podocytes with a combination of low-dose TZD + BX and studied this effect after exerting lipotoxic damage with palmitic acid (PA), taking as controls the recommended doses for both pioglitazone (TZD) and Bexarotene (BX).

#### 3.2.1. TZD and BX rescue the changes in glucose metabolism, insulin resistance and inflammation in podocytes treated with PA

In WT-control podocytes exposed to PA we found that that both BX or TZD independently, as well as the half-dose combination therapy (TZD + BX) reduced inflammation as shown by the decline in TNF $\alpha$  and PAI-1 expression after PA treatment (Fig. 8A).

Furthermore, these treatments were able to rescue the PA induced insulin resistance as evidenced by enhanced pAkt levels (Fig. 8B) and improved insulin stimulated GLUT4 membrane translocation (Fig. 8C).

#### 3.2.2. TZD and BX promote intracellular accumulation of palmitic acid in a small number of large lipid droplets in podocytes

PA promoted the formation of many small lipid droplets inside the WT-podocytes (Fig. 9A). However, when we treated with PA accompanied with BX or/and TZD, less but larger lipid drops were observed. This was checked by measurement and quantification of Bodipy staining (Fig. 9A) and by immunofluorescence of perilipin 2 (Fig. 9B).

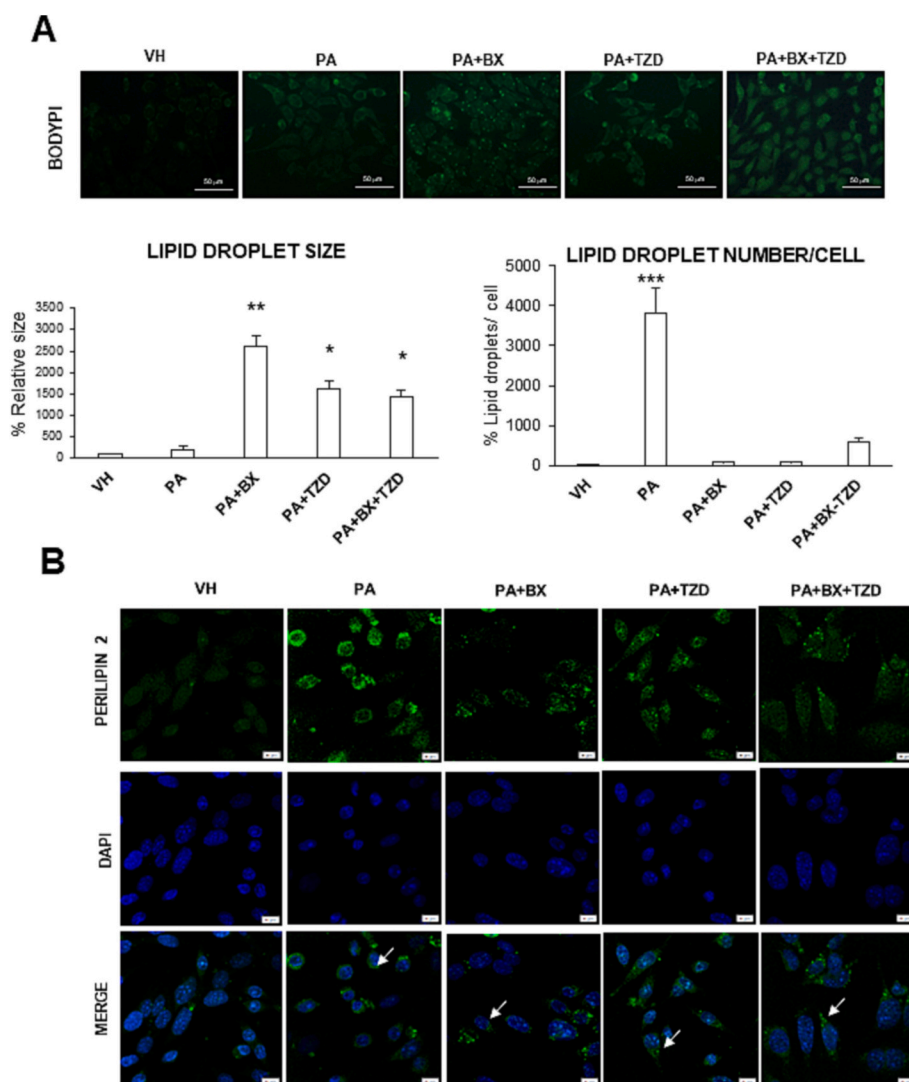


**Fig. 9.** TZD and BX promote intracellular accumulation of palmitic acid in a small number of large lipid droplets in podocytes. **A:** Representative BODYPI staining in podocytes and colour quantification after dye elution ( $n = 3$  experiments), original magnification:  $400\times$ . \* $p < 0.05$  versus VH; \*\* $p < 0.01$  vs. VH; \*\*\* $p < 0.001$  vs. VH. PA: Palmitic acid; BX: Bexarotene; TZD: Thiazolidinedione. **B:** Representative photographs of immunohistochemistry of Perilipin 2 ( $n = 3$  experiments); White arrows show perilipin 2 in lipid droplets inside podocytes Original magnification:  $400\times$ ; VH: Vehicle; PA: Palmitic acid; BX: Bexarotene; TZD: Thiazolidinedione.

### 3.2.3. TZD and BX decrease ER stress, ROS production and apoptosis in PA-treated podocytes

We observed that DHE fluorescence (a marker of superoxide production) was back to basal levels after treatment of PA + BX and combined treatment of PA + BX + TZD, but not after PA + TZD treatment alone (Fig. 10A). Moreover, the levels of ER stress were reversed in all three pharmacological treatments (Fig. 10B), as was shown by the presence of CHOP in the cytoplasm.

In addition, while treatments with BX or TZD alone were not able to significantly decrease apoptosis a combination of both agonists appeared to exert a synergistic effect, as it lowered apoptosis measured by flow cytometry through Annexin-V FITC and PI. Staining (Fig. 11A) and recovery of the antiapoptotic protein Bcl-2 level (Fig. 11B).

## 4. Discussion

PPAR $\gamma$  is a nuclear hormone receptor expressed in kidney podocytes. Our results show that PPAR $\gamma$  is essential for podocyte function since its deletion decreases levels of podocin and nephrin, two crucial proteins for correct formation of the slit diaphragm and for the maintenance of the glomerular filtration barrier. Furthermore, deletion of PPAR $\gamma$  promoted a dysregulation of nuclear receptors expression and lipid homeostasis, with lipid accumulation in the form of large lipid droplets. Moreover, PPAR $\gamma$ KO podocytes showed an increased basal level in ROS production, ER stress and a loss of cell viability due to increased

apoptosis. Despite all these effects, PPAR $\gamma$ KO podocytes lacked an inflammatory response and appeared to have improved insulin sensitivity.

These results lead us to speculate that PPAR $\gamma$  is essential for podocyte function and is a major regulator of lipid metabolism, through the accumulation of lipid droplets, reticulum stress and inflammation. The podocyte-specific deletion of PPAR $\gamma$  in mouse also shows a decrease in nephrin expression and develops proteinuria at 3 months of age [30,8].

We found that podocyte PPAR $\gamma$  deletion also caused a significant increase in the expression of RXR, its heterodimerization partner, most probably to compensate for the loss of PPAR $\gamma$  expression. This increase in RXR expression matched the appearance of large lipid droplets inside the cell of PPAR $\gamma$ KO podocytes. We also found these large lipid droplets in WT-control podocytes that had been stimulated with RXR and TZD agonists. The appearance of lipid droplets of a certain size could be related to the sensitivity of the cells to insulin. From our work large droplets were associated with insulin sensitive cells and those cells with more, smaller droplets were insulin resistant. Although there are studies that relate to the damage effect of lipid accumulation inside podocytes [31,32], in recent years an emerging opinion considers that lipid droplets can act in a bidirectional way, both as a sink of lipids to control cellular stress or as a source to produce lipid mediators [33]. The role of the lipid droplets within the podocyte is still unclear. In our study we show that they seemed to exhibit a protective mechanism since they stored an excess of lipids that could be harmful for the mitochondria, for example unfolded proteins or APOL1 risk variants as previously shown

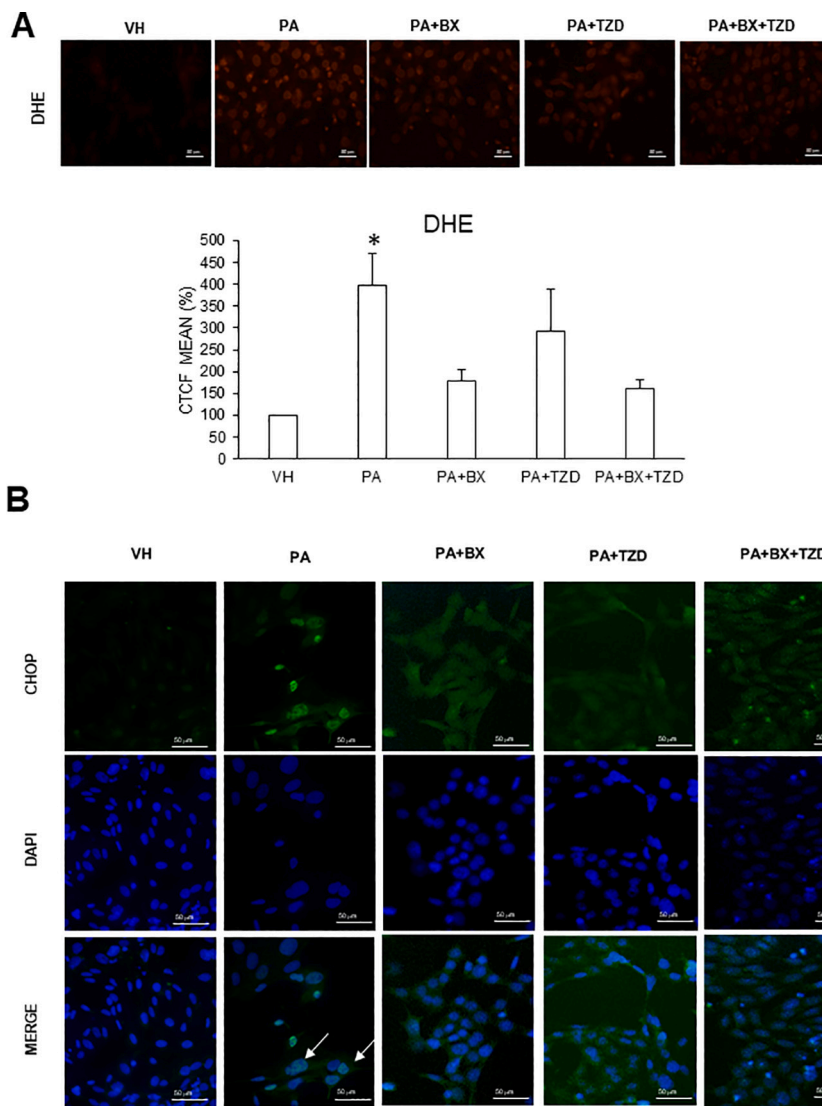


**Fig. 10.** TZD and BX decrease ER stress and ROS production in PA-treated podocytes. (A) Representative photographs of the nuclei of podocytes incubated with Di-hydroethidium (DHE) probe and red fluorescence quantification is expressed in arbitrary units (A.U.) ( $n = 3$  experiments),  $*p < 0.05$  versus VH; original magnification: 200 $\times$ ; (B) Representative micrographs of the immunofluorescence for c/EBP homologous protein (CHOP) in podocytes treated 24 h with VH, PA, TZD, BX or both (white arrows at stained nuclei). VH: Vehicle; PA: Palmitic acid; BX: Bexarotene; TZD: Thiazolidinedione. Magnification 400 $\times$ .

[34].

In addition, the PPAR $\gamma$ KO podocytes showed increased expression levels of nuclear receptors that heterodimerize with RXR such as VDR, FXR and RAR $\alpha$ . LXR $\alpha$  is the isoform of LXR receptor that is highly expressed in the kidney, liver, adipose tissue, intestine, and macrophages. This receptor is involved in preventing cellular cholesterol accumulation and has several coactivators including PGC-1 $\alpha$  [35]. In PPAR $\gamma$ KO podocytes we found a decrease in its coactivator PGC-1 $\alpha$  and LXR, probably related to the appearance of large lipid droplets in the cell. In the case of RAR, which heterodimerizes with RXR, it has been described that overexpression is related to liver damage and the forming of insoluble lipid droplets in the liver [35,36]. Further investigation is needed to determine which one is responsible and contributes in a higher degree to the lipid droplet formation.

In recent years, several studies have shown the benefits of vitamin D on kidney by its pleiotropic effects. In this regard, it has been seen that VDR activation has beneficial effects, such as antiproteinuric effect, due to direct protective action on the podocyte, decreasing inflammation, apoptosis, preserving mitochondrial morphology and modulating TGF $\beta$  in animal models of glomerular disease [37–39]. The increased VDR mRNA expression could also help to explain the lack of inflammation observed in PPAR $\gamma$ KO podocytes. Conversely, FXR is involved in lipid metabolism and inflammation [40]. It has been seen that FXR/RXR regulates CHOP expression, suggesting a beneficial and protective effect

of its activation [40]. This may explain why in PPAR $\gamma$ KO podocytes, which have constitutively high FXR expression, levels of CHOP did not decrease as they did in control podocytes after pharmacological treatment with TZD or BX.

Unexpectedly, we found that the PA treatment of PPAR $\gamma$ KO podocytes did not result in the development of insulin resistance compared to PA stimulated WT-control podocytes [41,42]. This may be explained as PPAR $\gamma$  mutations in humans and the deletion of PPAR $\gamma$  in murine models lead to the development of type 2 diabetes (T2D) [43,44]. However, murine PPAR $\gamma$  heterozygotes have improved insulin sensitivity [41,45,46] and are protected from the hepatic steatosis and renal injury induced by a high-fat diet [36]. Consistent with this, the human polymorphism Pro12Ala in PPAR $\gamma$ 2, which moderately reduces the transcriptional activity of PPAR $\gamma$ , has been shown to improve insulin sensitivity [46]. Our results showed that PPAR $\gamma$ KO podocytes lost the expression of RBP1, a protein involved in the transport of retinol [47], and RBP4, a protein that transports retinol in circulation and in both cases, the loss of their expression was related to increased insulin sensitivity. It has been shown that RBP1KO mice remain more glucose tolerant and insulin sensitive during high-fat-diet feeding [28,47]. Similarly RBP4-KO mice are more insulin sensitive and lowering RBP4 protects from HFD-induced insulin resistance [48,49]. These two proteins RBP1 and RBP4, along with RBP7 are target genes of PPAR $\gamma$  [27,28,50]. These results require more in-depth and future research.

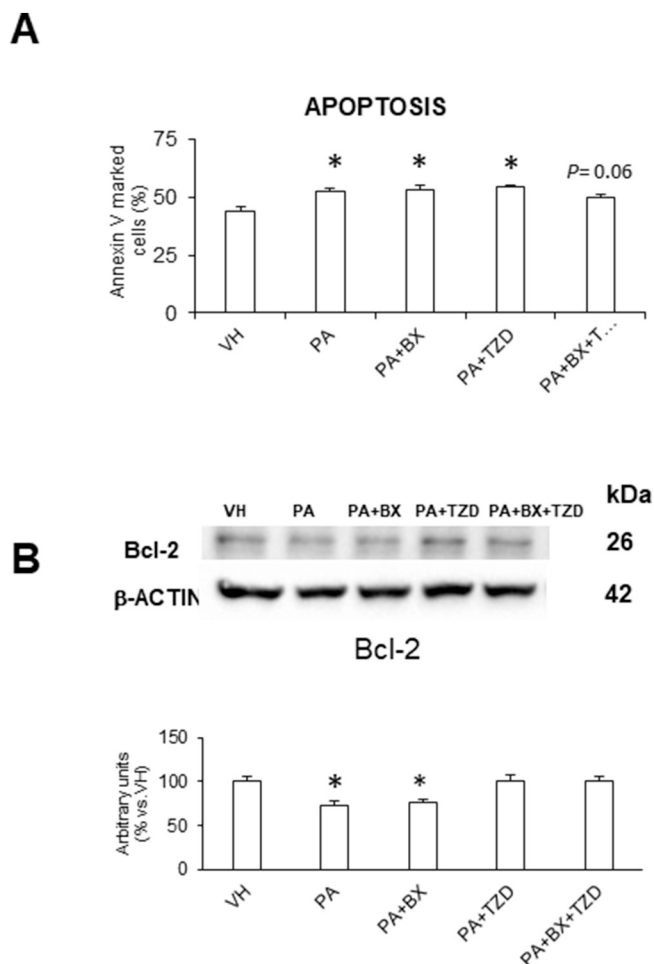


**Fig. 11.** Combined therapy of TZD and BX promoted a decline in apoptosis PA-induced in podocytes. A: Representation of percentage of cell death by apoptosis measured with annexin V by flow cytometry; B: Protein expression of antiapoptotic protein B-cell lymphoma 2 (Bcl-2). \* $p < 0.05$  versus VH.  $N = 3$  experiments.

Given the benefit that PPAR $\gamma$  seems to have in the podocyte and the nephroprotective effect of the activation of this nuclear receptor by its agonists TZDs [15,51], it has side effects limiting its use. For TZDs these include edema, osteoporosis, and bladder cancer [15]. For this reason, we tested the effect of Bexarotene (BX), a selective retinoid X receptor (RXR), which heterodimerizes with PPAR $\gamma$ . We found that BX treatment of PA damaged WT-control podocytes caused a significant increase in genes related to lipid synthesis. This increase was accompanied by a lack of recovery of ABCA1, a regulator of vesicular secretion of phospholipids and cholesterol [19,52,53], and an increase of Perilin2, which could explain why the treatment with BX promotes the formation of large lipid droplets observed in these cells. Conversely, the treatment with BX of WT-control PA-injured podocytes resulted in an increase in genes involved in  $\beta$ -oxidation of fatty acids. This was also observed to a lesser extent in PA WT-control treated with TZDs, leading to the decrease in oxidative stress shown in the treatments tested.

Our studies examining the combined use of low dose BX and TZD in PA podocyte damage agreed well with those who described the beneficial role of this combination in other situations [19,52,53]. Previously, the synergistic effect of BX and TZD has been proved to avoid the TZD tumorigenicity, which need to be added to the other desirable effects on inflammation and the vasculature, edema and weight gain. These data support the idea of using a combined therapy, which would allow reducing the dose of both agonists to potentially avoid their side effects. To the best of our knowledge, this is the first work where a combined

therapy has been tested in podocytes in this setting. Our results show that combination therapy reduced oxidative, ER stress and apoptosis while restoring insulin sensitivity after lipotoxic damage in podocytes. This is similar to the combination treatment with rexinoid and TZD that prevents insulin resistance in cells isolated from the liver of the HFD fed rabbits [54].

## 5. Conclusions

PPAR $\gamma$  is crucial for podocyte function. Here, PPAR $\gamma$  participates in the adaptation to lipid overload of these cells by inducing pathways for catabolism, utilization in biosynthetic pathways, and storage in lipid droplets. PPAR $\gamma$  deletion leads to a dysregulation of the expression of other nuclear receptors, mainly RXR. Treatment with low-dose combined therapy of PPAR $\gamma$  and RXR agonists has a protective effect for the podocyte and appears to act synergistically on these cells. The use of a combination therapy of TZD and RXR agonists could be an alternative for the treatment of kidney disease associated to obesity. However, further investigation is needed to understand the dependence between different nuclear receptors. This would allow reducing the doses of the drugs and potentially reduce their side effects to enhance the recovery of the internal lipid balance and to improve the inflammatory state of the podocyte.

Supplementary data to this article can be found online at <https://doi.org/10.1016/j.bbalip.2023.159329>.

## Funding

Research conducted for this publication was supported by the Mobility stays abroad José Castillejo for young doctors of Ministerio de Educación Cultura y Deporte de España [CAS 12/00160], Ministerio de Economía y Competitividad de España [BFU2016-78951-R, BFU2017-90578-REDT], Ministerio de Ciencia e Innovación [PID2020-116875RB-I00], Comunidad de Madrid (Spain) [S2017/BMD-3684, P2022/BMD-7227]. RJC was supported by the British Medical Research Council (MRC) with a Senior Clinical Fellowship [MR/K010492/1].

## Institutional review board statement

All animal protocols used in this study were approved by the Research Ethics Committee of the Universidad Rey Juan Carlos.

## CRedit authorship contribution statement

AIL, AGG and GMG designed the study; AGC, AIL, LN, EFS and AMV performed the experiments; AGC and AIL analyzed the data; AGC and AIL prepared the figures; AGC, AIL, AMV, RC and GMG drafted and revised the paper. All authors approved the final version of the manuscript.

## Declaration of competing interest

The authors declare the following financial interests/personal relationships which may be considered as potential competing interests:

Adriana Izquierdo-Lahuerta reports travel was provided by Ministerio de Educación Cultura y Deporte. Gema Medina-Gomez reports financial support was provided by Ministerio de Economía y Competitividad de España. Gema Medina-Gomez reports financial support was provided by Community of Madrid Health Service. Richard J. Coward reports financial support was provided by British Medical Research Council.

## Data availability

No data was used for the research described in the article.



## Acknowledgments

We thank Frank J Gonzalez (Laboratory of Metabolism, National Cancer Institute, National Institutes of Health, Bethesda, MD, USA) by donated the PPAR $\gamma$ floxed mice and Jose Antonio Más and Alexander Otero for their excellent technical support.

## References

- [1] G. Medina-Gomez, S.L. Gray, L. Yetukuri, K. Shimomura, S. Virtue, M. Campbell, R. K. Curtis, M. Jimenez-Linan, M. Blount, G.S.H. Yeo, M. Lopez, T. Seppänen-Laakso, F.M. Ashcroft, M. Orešić, A. Vidal-Puig, PPAR  $\gamma$  2 prevents lipotoxicity by controlling adipose tissue expandability and peripheral lipid metabolism, *PLoS Genet.* 3 (4) (2007) 0634–0647, <https://doi.org/10.1371/journal.pgen.0030064>.
- [2] E.D. Rosen, P. Sarraf, A.E. Troy, G. Bradwin, K. Moore, D.S. Milstone, B. M. Spiegelman, R.M. Mortensen, D. Farber, *PPAR Functions* 4, 1999.
- [3] C. Platt, R.J. Coward, Peroxisome proliferator activating receptor- $\gamma$  and the podocyte, in: *Nephrology Dialysis Transplantation*, 2017, pp. 423–433, <https://doi.org/10.1093/ndt/gfw320>.
- [4] P. Corrales, A. Izquierdo-Lahuerta, G. Medina-Gómez, Maintenance of kidney metabolic homeostasis by PPAR gamma, *Int. J. Mol. Sci.* 19 (7) (2018), <https://doi.org/10.3390/ijms19072063>.
- [5] C. Martínez-García, A. Izquierdo, V. Velagapudi, Y. Vivas, I. Velasco, M. Campbell, K. Burling, F. Cava, M. Ros, M. Oresic, A. Vidal-Puig, G. Medina-Gomez, Accelerated renal disease is associated with the development of metabolic syndrome in a glucolipotoxic mouse model, *Dis. Model. Mech.* 5 (5) (2012) 636–648, <https://doi.org/10.1242/dmm.009266>.
- [6] A. Falkevall, A. Mehlem, I. Palombo, B. Heller Sahlgren, L. Ebarasi, L. He, A. J. Ytterberg, H. Olauson, J. Axelsson, B. Sundelin, J. Patrakka, P. Scotney, A. Nash, U. Eriksson, Reducing VEGF-B signaling ameliorates renal lipotoxicity and protects against diabetic kidney disease, *Cell Metab.* 25 (3) (2017) 713–726, <https://doi.org/10.1016/j.cmet.2017.01.004>.
- [7] C. Martínez-García, A. Izquierdo-Lahuerta, Y. Vivas, I. Velasco, T.-K. Yeo, S. Chen, G. Medina-Gomez, Renal lipotoxicity-associated inflammation and insulin resistance affects actin cytoskeleton Organization in Podocytes, *PLoS One* 10 (11) (2015), e0142291, <https://doi.org/10.1371/journal.pone.0142291>.
- [8] C. Henique, G. Bollee, O. Lenoir, N. Dhaun, M. Camus, A. Chipont, K. Flosseau, C. Mandet, M. Yamamoto, A. Karras, E. Therivet, P. Bruneval, D. Nochy, L. Mesnard, P.-L. Tharaux, Nuclear factor erythroid 2-related factor 2 drives podocyte-specific expression of peroxisome proliferator-activated receptor  $\gamma$  essential for resistance to crescentic GN, *J. Am. Soc. Nephrol.* 27 (1) (2016), <https://doi.org/10.1681/ASN.2014111080>.
- [9] Y. Zuo, H.C. Yang, S.A. Potthoff, B. Najafian, V. Kon, L.J. Ma, A.B. Fogo, Protective effects of PPAR $\gamma$  agonist in acute nephrotic syndrome, *Nephrol. Dial. Transplant.* 27 (1) (2012) 174–181, <https://doi.org/10.1093/ndt/gfr240>.
- [10] J.E. Toblli, M.G. Ferrini, G. Cao, D. Vernet, M. Angerosa, N.F. Gonzalez-Cadavid, Antifibrotic effects of pioglitazone on the kidney in a rat model of type 2 diabetes mellitus, *Nephrol. Dial. Transplant.* 24 (8) (2009) 2384–2391, <https://doi.org/10.1093/ndt/gfp103>.
- [11] T. Kanjanabuch, L.J. Ma, J. Chen, A. Pozzi, Y. Guan, P. Mundel, A.B. Fogo, PPAR- $\gamma$  agonist protects podocytes from injury, *Kidney Int.* 71 (12) (2007) 1232–1239, <https://doi.org/10.1038/sj.ki.5002248>.
- [12] F. Kindt, E. Hammer, S. Kemnitz, A. Blumenthal, P. Klemm, R. Schlüter, S. E. Quaggin, J. van den Brandt, G. Fuellen, U. Völker, K. Endlich, N. Endlich, A novel assay to assess the effect of pharmaceutical compounds on the differentiation of podocytes, *Br. J. Pharmacol.* 174 (2) (2017) 163–176, <https://doi.org/10.1111/bph.13667>.
- [13] G. Miglio, A.C. Rosa, L. Rattazzi, C. Grange, G. Camussi, R. Fantozzi, Protective effects of peroxisome proliferator-activated receptor agonists on human podocytes: proposed mechanisms of action, *Br. J. Pharmacol.* 167 (3) (2012) 641–653, <https://doi.org/10.1111/j.1476-5381.2012.02026.x>.
- [14] S. Agrawal, J.C. He, P.L. Tharaux, Nuclear receptors in podocyte biology and glomerular disease, *Nat Rev Nephrol* 17 (3) (2021) 185–204, <https://doi.org/10.1038/s41581-020-00339-6>.
- [15] H.E. Lebovitz, Thiazolidinediones: the forgotten diabetes medications, in: *Current Diabetes Reports*, Springer, December 1, 2019, <https://doi.org/10.1007/s1892-019-1270-y>.
- [16] S. Agrawal, M.A. Chanley, D. Westbrook, X. Nie, T. Kitao, A.J. Guess, R. Benndorf, G. Hidalgo, W.E. Smoyer, Pioglitazone enhances the beneficial effects of glucocorticoids in experimental nephrotic syndrome, *Sci. Rep.* (2016) 6, <https://doi.org/10.1038/srep24392>.
- [17] K. Matsushita, H.C. Yang, M.M. Mysore, J. Zhong, Y. Shyr, L.J. Ma, A.B. Fogo, Effects of combination PPAR $\gamma$  agonist and angiotensin receptor blocker on glomerulosclerosis, *Lab. Invest.* 96 (6) (2016) 602–609, <https://doi.org/10.1038/labinvest.2016.42>.
- [18] E. Han, E. Shin, G. Kim, J.Y. Lee, B.W. Lee, E.S. Kang, B.S. Cha, Lee Y. Ho, Combining SGLT2 inhibition with a thiazolidinedione additively attenuate the very early phase of diabetic nephropathy progression in type 2 diabetes mellitus, *Front Endocrinol (Lausanne)* 9 (JUL) (2018), <https://doi.org/10.3389/fendo.2018.00412>.
- [19] S. de Flora, G. Ganchev, M. Ilcheva, S. la Maestra, R.T. Micale, V.E. Steele, R. Balansky, Pharmacological modulation of lung carcinogenesis in smokers: preclinical and clinical evidence, *Trends in Pharmacological Sciences.* (February 1, 2016) 120–142, <https://doi.org/10.1016/j.tips.2015.11.003>. Elsevier Ltd.
- [20] A. Izzotti, R. Balansky, F. D'Agostini, M. Longobardi, C. Cartiglia, S. la Maestra, R. T. Micale, A. Camoirano, G. Ganchev, M. Ilcheva, V.E. Steele, S. de Flora, Relationships between pulmonary micro-rna and proteome profiles, systemic cytogenetic damage and lung tumors in cigarette smoke-exposed mice treated with chemopreventive agents, *Carcinogenesis* 34 (10) (2013) 2322–2329, <https://doi.org/10.1093/carcin/bgt178>.
- [21] T.E. Akiyama, S. Sakai, G. Lambert, C.J. Nicol, K. Matsusue, S. Pimprale, Y.-H. Lee, M. Ricote, C.K. Glass, H.B. Brewer, F.J. Gonzalez, Conditional disruption of the peroxisome proliferator-activated receptor  $\gamma$  gene in mice results in lowered expression of ABCA1, ABCG1, and ApoE in macrophages and reduced cholesterol efflux, *Mol. Cell. Biol.* 22 (8) (2002) 2607–2619, <https://doi.org/10.1128/mcb.22.8.2607-2619.2002>.
- [22] M.A. Saleem, M.J. O'hare, J. Reiser, R.J. Coward, C.D. Inward, T. Farren, C.Y. Xing, L. Ni, P.W. Mathieson, P. Mundel, A Conditionally Immortalized Human Podocyte Cell Line Demonstrating Nephritin and Podocin Expression, 2002.
- [23] L. Ni, M. Saleem, P.W. Mathieson, Podocyte culture: tricks of the trade, *Nephrology (Carlton)* 6 (2012) 525–531, <https://doi.org/10.1111/j.1440-1797.2012.01619.x>.
- [24] M.W. Pfaffl, A. Tichopad, C. Prgomet, T.P. Neuvians, Determination of Stable Housekeeping Genes, Differentially Regulated Target Genes and Sample Integrity: BestKeeper-Excel-Based Tool Using Pair-Wise Correlations 26, 2004. <http://www.wzw.tum.de/gene-quantification/bestkeeper.html>.
- [25] F. Jiménez-Altayó, A.M. Briones, J. Giraldo, A.M. Planas, M. Salices, E. Vila, Increased superoxide anion production by interleukin-1 $\beta$  impairs nitric oxide-mediated relaxation in resistance arteries, *J. Pharmacol. Exp. Ther.* 316 (1) (2006) 42–52, <https://doi.org/10.1124/jpet.105.088435>.
- [26] M. Kauffman, M. Kauffman, K. Traore, H. Zhu, M. Trush, Z. Jia, Y. Li, MitoSOX-based flow cytometry for detecting mitochondrial ROS, Reactive Oxygen Species (2016), <https://doi.org/10.20455/ros.2016.865>.
- [27] C.F. Zizola, G.J. Schwartz, S. Vogel, Cellular retinol-binding protein type III is a PPAR $\gamma$  target gene and Plays a role in lipid metabolism, *Am. J. Physiol. Endocrinol. Metab.* 295 (6) (2008) 1358–1368, <https://doi.org/10.1152/ajpendo.90464.2008>.
- [28] C.F. Zizola, S.K. Frey, S. Jitngarmkusol, B. Kadereit, N. Yan, S. Vogel, Cellular retinol-binding protein type I (CRBP-I) regulates adipogenesis, *Mol. Cell. Biol.* 30 (14) (2010) 3412–3420, <https://doi.org/10.1128/mcb.00014-10>.
- [29] M. Rosell, E. Hondares, S. Iwamoto, F.J. Gonzalez, M. Wabitsch, B. Staels, Y. Olmos, M. Monsalve, M. Giral, R. Iglesias, F. Villarroya, Peroxisome proliferator-activated receptors- $\alpha$  and - $\gamma$  and CAMP-mediated pathways, control retinol-binding protein-4 gene expression in brown adipose tissue, *Endocrinology* 153 (3) (2012) 1162–1173, <https://doi.org/10.1210/en.2011-1367>.
- [30] R. Sonneveld, J.G. Hoenderop, A.M. Isidori, C. Henique, H.B. Dijkman, J. H. Berden, P.L. Tharaux, J. van der Vlag, T. Nijenhuis, Sildenafil prevents podocyte injury via PPAR-g-mediated TRPC6 inhibition, *J. Am. Soc. Nephrol.* 28 (5) (2017) 1491–1505, <https://doi.org/10.1681/ASN.2015080885>.
- [31] J. Zhao, H.L. Rui, M. Yang, L.J. Sun, H.R. Dong, H. Cheng, CD36-mediated lipid accumulation and activation of NLRP3 inflammasome Lead to podocyte injury in obesity-related glomerulopathy, *Mediat. Inflamm.* 2019 (2019), <https://doi.org/10.1155/2019/3172647>.
- [32] Y. Zhang, K.L. Ma, J. Liu, Y. Wu, Z.B. Hu, L. Liu, J. Lu, X.L. Zhang, B.C. Liu, Inflammatory stress exacerbates lipid accumulation and podocyte injuries in diabetic nephropathy, *Acta Diabetol.* 52 (6) (2015) 1045–1056, <https://doi.org/10.1007/s00592-015-0753-9>.
- [33] E. Jarc, T. Petan, A twist of FATE: lipid droplets and inflammatory lipid mediators, *Biochimie* 169 (2020) 69–87, <https://doi.org/10.1016/j.biochi.2019.11.016>.
- [34] Y. Sun, S. Cui, Y. Hou, F. Yi, The updates of podocyte lipid metabolism in proteinuric kidney disease, *Kidney Dis.* 7 (6) (2021) 438–451, <https://doi.org/10.1159/000518132>.
- [35] A. Saeed, P. Bartuzi, J. Heegsma, D. Dekker, N. Kloosterhuis, A. de Bruin, J. W. Jonker, B. van de Sluis, K.N. Faber, Impaired hepatic vitamin a metabolism in NAFLD mice leading to vitamin a accumulation in hepatocytes, *CMGH* 11 (1) (2021) 309–325.e3, <https://doi.org/10.1016/j.jcmgh.2020.07.006>.
- [36] M.S. Abdel-Bakky, M.A. Hammad, L.A. Walker, M.K. Ashfaq, Tissue factor dependent liver injury causes release of retinoid receptors (RXR- $\alpha$  and RAR- $\alpha$ ) as lipid droplets, *Biochem. Biophys. Res. Commun.* 410 (1) (2011) 146–151, <https://doi.org/10.1016/j.bbrc.2011.05.127>.
- [37] M. Vanessa Pérez-Gómez, A. Ortiz-Ardúa, V. Lorenzo-Sellares, Vitamina D y proteinuria: Revisión Crítica de las bases moleculares y de La experiencia Clínica, *Nefrologia* 33 (5) (2013) 716–726, <https://doi.org/10.3265/Nefrologia.pre2013.Apr.12025>.
- [38] M.-D. Sanchez-Niño, M. Bozic, E. Córdoba-Lanús, P. Valcheva, O. Gracia, M. Ibarz, E. Fernandez, J.F. Navarro-Gonzalez, A. Ortiz, J.M. Valdivielso, Beyond proteinuria: VDR activation reduces renal inflammation in experimental diabetic nephropathy, *Am J Physiol Renal Physiol* 302 (2012) 647–657, <https://doi.org/10.1152/ajprenal.00090.2011-Local>.
- [39] G. Gembillo, R. Siligato, M. Amatruda, G. Conti, D. Santoro, Vitamin D and glomerulonephritis, *Medicina (Lithuania)* (February 1, 2021) 1–15, <https://doi.org/10.3390/medicina57020186>. MDPI AG.
- [40] C.D. Fuchs, T. Claudel, H. Scharnagl, T. Stojakovic, M. Trauner, FXR controls CHOP expression in steatohepatitis, *FEBS Lett.* 591 (20) (2017) 3360–3368, <https://doi.org/10.1002/1873-3468.12845>.
- [41] S. Kume, T. Uzu, T. Sugimoto, K. Isshiki, M. Chin-Kanasaki, M. Sakaguchi, N. Kubota, Y. Terauchi, T. Kadowaki, M. Haneda, A. Kashiwagi, D. Koya, S.-I. Araki, Role of altered renal lipid metabolism in the development of renal injury induced by a high-fat diet, *Journal of the American Society of Nephrology* 18 (10) (2007) 2715–2723, <https://doi.org/10.1681/ASN.2007010089>.



- [42] Philip D.G. Miles, Yaacov Barak, Weiman He, Ronald M. Evans, Jerrold M. Olefsky, Improved insulin-sensitivity in mice heterozygous for PPAR- $\gamma$  deficiency, *J Clin Invest* 105 (3) (2000).
- [43] B. Toffoli, F. Gilardi, C. Winkler, M. Soderberg, L. Kowalczyk, Y. Arsenijevic, K. Bamberg, O. Bonny, B. Desvergne, Nephropathy in ppar $\gamma$ -null mice highlights PPAR $\gamma$  systemic activities in metabolism and in the immune system, *PLoS One* 12 (2) (2017), <https://doi.org/10.1371/journal.pone.0171474>.
- [44] F. Gilardi, C. Winkler, L. Quignodon, J.G. Diserens, B. Toffoli, M. Schiffrin, C. Sardella, F. Preitner, B. Desvergne, Systemic PPAR $\gamma$  deletion in mice provokes lipotrophy, organomegaly, severe type 2 diabetes and metabolic inflexibility, *Metabolism* 95 (2019) 8–20, <https://doi.org/10.1016/j.metabol.2019.03.003>.
- [45] J. Rieusset, F. Touri, L. Michalik, P. Escher, B. Desvergne, E. Niesor, W. Wahli, A new selective peroxisome proliferator-activated receptor  $\gamma$  antagonist with antiobesity and antidiabetic activity, *Mol. Endocrinol.* 16 (11) (2002) 2628–2644, <https://doi.org/10.1210/me.2002-0036>.
- [46] S.S. Deeb, L. Fajas, M. Nemoto, J. Pihlajamäki, L. Mykkänen, J. Kuusisto, M. Laakso, W. Fujimoto, J. Auwerx, A Pro12Ala Substitution in PPAR $\gamma$ 2 Associated With Decreased Receptor Activity, Lower Body Mass Index and Improved Insulin Sensitivity. <http://genetics.nature.com>.
- [47] G. Carta, E. Murru, L. Cordeddu, B. Ortiz, E. Giordano, M.A. Belury, L. Quadro, S. Banni, Metabolic interactions between vitamin a and conjugated linoleic acid, *Nutrients*. MDPI AG (March 24, 2014) 1262–1272, <https://doi.org/10.3390/nu6031262>.
- [48] Y. Tan, L.Q. Sun, M.A. Kamal, X. Wang, J.P. Seale, X. Qu, Suppression of retinol-binding protein 4 with RNA oligonucleotide prevents high-fat diet-induced metabolic syndrome and non-alcoholic fatty liver disease in mice, *Biochim. Biophys. Acta Mol. Cell Biol. Lipids* 1811 (12) (2011) 1045–1053, <https://doi.org/10.1016/j.bbali.2011.09.011>.
- [49] B.J. Kraus, J.L. Sartoretto, P. Polak, T. Hosooka, T. Shiroto, I. Eskurza, S.-A. Lee, H. Jiang, T. Michel, B.B. Kahn, Novel role for retinol-binding protein 4 in the regulation of blood pressure, *FASEB J.* 29 (8) (2015) 3133–3140, <https://doi.org/10.1096/fj.14-266064>.
- [50] D.H. Kim, J. Ahn, Y. Suh, O. Ziouzenkova, J.W. Lee, K. Lee, Retinol binding protein 7 promotes adipogenesis in vitro and regulates expression of genes involved in retinol metabolism. *Front cell, Dev. Biol.* (2022) 10, <https://doi.org/10.3389/fcell.2022.876031>.
- [51] G. Bansal, P.V. Thanikachalam, R.K. Maurya, P. Chawla, S. Ramamurthy, An overview on medicinal perspective of Thiazolidine-2,4-Dione: a remarkable scaffold in the treatment of type 2 diabetes, *J. Adv. Res.* 23 (2020) 163–205, <https://doi.org/10.1016/j.jare.2020.01.008>.
- [52] J.P. Klopffer, V. Sharma, A. Berenz, W.R. Hays, M. Loi, U. Pugazhenth, S. Said, B. R. Haugen, Retinoid and thiazolidinedione therapies in melanoma: an analysis of differential response based on nuclear hormone receptor expression, *Mol Cancer* 8 (2009), <https://doi.org/10.1186/1476-4598-8-16>.
- [53] S. La Maestra, R.T. Micale, S. de Flora, F. D'agostini, G. Ganchev, M. Ilcheva, N. Petkov, V.E. Steele, R. Balansky, DNA damage in exfoliated cells and histopathological alterations in the urinary tract of mice exposed to cigarette smoke and treated with chemopreventive agents, *Carcinogenesis* 34 (1) (2013) 183–189.
- [54] E. Maneschi, L. Vignozzi, A. Morelli, T. Mello, S. Filippi, I. Cellai, P. Comeglio, E. Sarchielli, A. Calcagno, B. Mazzanti, R. Vettor, G.B. Vannelli, L. Adorini, M. Maggi, FXR activation normalizes insulin sensitivity in visceral preadipocytes of a rabbit model of mets, *J. Endocrinol.* 218 (2) (2013) 215–231, <https://doi.org/10.1530/JOE-13-0109>.